DfR Solutions
reliability designed, reliability delivered

White Paper

Solder Phase Coarsening, Fundamentals, Preparation, Measurement and Prediction

5110 Roanoke Place, Suite 101 College Park, Maryland 20740
Phone (301) 474-0607 Fax (240) 757-0053
www.DfRSolutions.com

Solder Phase Coarsening, Fundamentals, Preparation, Measurement and Prediction

Crina Rauta, Dr. Abhijit Dasgupta and Dr. Craig Hillman

DfR Solutions
College Park, MD 20740

Abstract. Thermal fatigue has been one of the most serious problems for solder joint reliability. Thermo-mechanical fatigue failure is considered to be closely related to micro-structural coarsening (grain/phase growth). Factors that influence the phase growth are studied and measurement methods are discussed, including the preparation of the eutectic solder sample for phase size measurement. Three categories of models used to predict grain growth in polycrystalline materials are presented. Finally, phase growth in solder during high temperature aging and temperature cycling and its use as a damage correlation factor are discussed.

INTRODUCTION

In many applications, especially automotive, solder interconnects experience degradation due to prolonged temperature and power cycling. This degradation behavior manifests itself as changes in the grain structure, primarily through grain coarsening. Because the magnitude of the change in grain structure is strongly dependent upon the environmental stresses, quantifying microstructural changes provides an alternative approach to calculating an acceleration transform number or function. FUND

FUNDAMENTALS OF GRAIN AND PHASE COARSENING

There are two fundamental forces that drive grains in polycrystalline materials to grow. Grains coarsen because grain boundaries are areas of high potential energy. This is the primary driving force in single-phase materials. During grain coarsening, as grains grow larger, the total grain boundary area decreases, which, in turn lowers the free energy of the system. Particles with smaller size tend to combine into a larger particle one with lower total interfacial energy. Grain growth is driven by the local boundary curvature and the presence of triple junctions, which remain in equilibrium and act as anchors to grain boundary mobility [1]. Grain boundary mobility is highly dependent upon grain orientations across the boundary.

In multiphase systems, the thermodynamic basis of phase coarsening is a combination of the driving force for grain coarsening and the Thomson-Freundlich solubility relationship [2]. According to this relationship, the solute concentration in the matrix adjacent to a particle will increase as the radius of curvature of the interface decreases. Thus, the solubility in the matrix in contact with a β particle increases as the radius of the β particle decreases. This results in the formation of concentration gradients n the matrix, which cause the solute to diffuse in the direction of the largest particles and away from the smallest particles. As the flow of solute proceeds, the small particles dissolve to compensate for the decrease in concentration at their interface. Likewise, the solute migrating towards the larger particles will precipitate at the particles and remove the excess solute arriving as the diffusion flux. Consequently, phase coarsening causes small particles to shrink and large particles to grow. This competitive growth and dislocation process will continue in theory, until the system is finally phase separated.

Factors and conditions that influence grain grow

Grain growth, also known as Ostwald ripening, is strongly influenced by the initial distributions of grain size and shape, the size, shape and distribution of the secondary or tertiary phases, and the dislocation density. These microstructural elements are

governed by a number of factors, including the composition of the alloy, the solubility of the various elements that comprise the alloy material, and the rate of cooling during solidification.

Because grain boundaries are areas of high potential energy, due to dangling atomic bonds, there is always a driving force for grain growth in all polycrystalline materials. The limiting factor is the application of sufficient thermal or mechanical energy to induce grain growth to occur at a measurable rate. High temperatures supply thermal energy and mechanical energy is supplied by the application of stress, both cyclic and static. The rate of grain coarsening increases with application of thermal energy, because increased diffusion allows for more rapid movement of grain boundaries. Coarsening due to the application of mechanical energy occurs when the stress levels result in plastic deformation. Plastic deformation results in the production of an excess concentration of vacancies, which creates additional paths for material transport across phase boundaries. In binary alloys, coarsening during temperature cycling below the eutectic may also occur because of changes in the miscibility of the two phases [3].

PREPARING EUTECTIC SOLDER FOR PHASE GROWTH MEASUREMENT

There are two methods for revealing phases in eutectic solder: polishing and etching.

Polishing of solder

Because of the very low hardness of eutectic solder, materials such as silicon carbide (SiC) and alumina (Al_2O_3) can be used for sample preparation. After using cutting wheels or coarser grit to reach the area of interest, 600 grit SiC can be used to prepare the cross-section. During grinding, the water is the lubrication medium of choice and the time required is approximately 30 to 60 seconds. The second and final step in grinding is 1200 grit to remove any damage remaining from the application of 600 grit.

Polishing of solder is often a two-step process. The first step involves polishing with a 1.0 or 0.3-micron size alumina powder suspended in distilled water. This step takes approximately 60-120 seconds and is completed when no surface damage, such as scratches, are visible. The second step consists of either 0.05-micron alumina or colloidal silica. Both polishing media attack the lead-rich and tin-rich regions at different rates, greatly increasing the microstructural contrast. The advantage of this process is that it is relatively simple involving non-toxic materials. The primary disadvantage of preferential polishing is that the time required creating the necessary contrast between the lead-rich and tin-rich regions can be on the order of five to ten minutes.

Etching of solder

There are a range of etchant compositions to choose from when attempting to reveal the microstructure of tin/lead and other tin-based alloys. A comprehensive list is displayed in Table 1. While compositions and recommended etch times can vary, the etchants can be broken down into recognizable categories.

The first category uses a strong acid, such as nitric acid, hydrochloric acid, or a combination of the two, highly diluted in a carrier liquid, such as a solvent or water[1].

The second category uses a weaker etchant, such as acetic acid, hydrogen peroxide, or ammonium hydroxide, to attack the grain boundaries. The first two categories are designed to primarily attack different parts of the material (grain boundaries vs. grains, lead-rich vs. tin-rich) at different rates.

The last category of etchants contains a material, such as ferric chloride or silver nitrate, which stains different parts of the alloy.

The primary advantage of etching is flexibility and efficiency. Different etchants will reveal different aspects of the microstructure, allowing the metallurgist to observe grain size, intermetallics, or some combination of the two. In addition,

[1] Use of deionized water reduces variability in etching process.

results are obtained much quicker when a large number of samples need to be inspected. The disadvantage of etching is controlling the etching process. Etching is often an iterative process, with a number of rounds of polishing, etching, re-polishing, and re-etching before the desired results are obtained. Etchant strength also tends to breakdown over time, so etchants should be used soon after they are mixed. In addition, there are always the health and environmental concerns over using hazardous chemicals.

Composition	**Etchant**	*Application* **Time**	**Reference**
Single Acid Etchants			
Pure Sn	HCl (2 parts), Ethanol or Methanol (98 parts)	Undefined	[4]
Sn/Pb, Sn/Sb/Cu	HCl (2-5 parts), Ethanol, Methanol or DI water (100 parts)	1-3 minutes	[5]
Lead-Free (microstructure)	HCl (10 parts), Methanol (90 parts)	2-5 sec	[6]
Sn/Ag/Cu, Sn/Sb	HNO_3 (2 parts), Isopropanol (98 parts)	3 sec	[7]
Sn/Sb	HNO_3 (2 parts), Ethanol or Methanol (98 parts)	Undefined	[4]
Double Acid Etchants			
Sn/Pb and all Sn alloys	HCl (2 parts), HNO_3 (5 parts), Methanol (93 parts)	Undefined	[4]
Sn/Ag, Sn/Bi, Sn/In, Sn/Sb/Cu	HCL (2 parts), HNO_3 (5 parts), Isopropanol (93 parts)	2 to 5 sec	[7]
Sn/Pb	Acetic Acid (3 parts), HNO_3 (4 parts), Deionized Water (16 parts)	5 - 15 sec	[7]
Sn/Pb (solder joints)	Acetic Acid (3 parts), HNO_3 (4 parts), Water (16 parts)	Undefined	[4]
Sn-rich Sn/Pb	Acetic Acid (1 part), HNO_3 (1 part), Glycerol (8 parts)	Undefined	[4]
Lead-Free (intermetallic)	Acetic Acid (1 part), HNO_3 (1 part), Glycerol (4 parts)	Undefined at 80°C	[6]
Other Etchant Compositions			
Sn alloys	Ferric Chloride (2 grams), HCl (5 ml) Water (30 ml) Ethanol or Methanol (60 ml)	Undefined	[4]
Sn/Cu	Ferric Chloride (10 grams), HCl (5-25 ml) Methanol or DI water (100 ml)	10 – 90 sec	[5]
Sn/Pb	3% H_2O_2 (25 parts), 28% NH_4OH (25 parts) Deionized Water (10 parts)	15 - 45 sec.	[7]
Sn coatings	30% H_2O_2 (few drops), NH_4OH (undefined amount)	Undefined	[4]
Pb-rich Sn/Pb	$AgNO_3$ (5 parts), Water (95 parts)	Undefined	[4]

Table 1 Etchants for tin/lead or other tin based alloysGRAIN/Phase GROWTH MEASUREMENT METHODS

Traditionally, there have been two methods for measuring the grain size: the line intercept method and the planimetric method. Both use an averaging technique to determine grain size. More recent methods, using the recent introduction of automated and semi-automated image analysis, allow for the measurements of individual grains and the acquisition of distribution information.

Line Intercept Method

Grain sizes are calculated from the mean intercept lengths between grain boundaries and the selected measurements line pattern. Horizontal, vertical, diagonal or circular line patterns as well as combinations thereof may be used. The procedure is to draw a line of length of length L or a circle of circumference L randomly on the microstructure and count the number of grains,

N, intercepted by the line (see Figure 1a). All whole grains intercepted are counted as 1 while grains at the end of the lines are counted as 1/2. The average grain size, *D*, can be found by dividing *L* by *N:*

$$D=L/N$$

The average of several values of *D* often gives a fairly accurate average grain size for the sample being measured [8].

Planimetric method

This approach measures grain size in terms of the number of grains visible on a cross section within a fixed area (see Figure 1b). The standard output is given in either the number of grains per square millimeter or the number of grains per square inch at 100x, which is related to the ASTM grain size number by

$$n = 2^{G-1}$$

where *n* is the number of grains per square inch at 100x magnification and *G* is the ASTM grain size number [10]. From this value, the average cross-sectional area of the bisected grains can be computed. This is not an average of the maximum cross-sectional area of each grain because the sectioning plane does not intersect each grain at its maximum width.

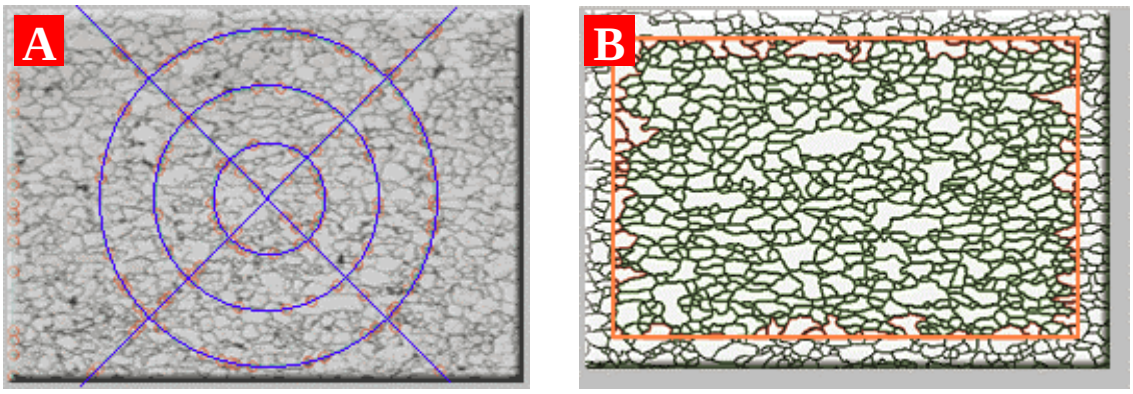

Figure 1 (A) Example of the linear intercept method. (B) Planimetric grain size measurements on a reconstructed grain image.

Comparison of the measurement methods

When using manual measurement methods, the essential goal is a balance of accuracy and efficiency. ASTM Method E 112 states that the intercept method is more convenient comparing to the planimetric method, which needs to mark off the grains for an accurate count. Intercept procedures are recommended particularly for all structures that depart from the uniform equiaxed form. [9] Future revisions will provide instructions for measuring the grain size of samples with deformed grains.

Ensuring the accuracy of grain size measurements is complicated by a number of factors. First, the three-dimensional size of the grains is not constant and the sectioning plane will cut through the grains at random. Thus, on a particular cross-section, only a very small percentage of grains will reveal their maximum dimension. Grain shape also varies, particularly as a function of grain size and thermal history. If the grain shape is highly anisotropic and the grain orientation is ordered, such is in the lamellar structure found in slow-cooled eutectic solder, this can lead to large errors in measurement. Second, is the different measures of grain size, which further complicates the accuracy of the measurement. The planimetric method, yields the number of grains per square millimeter area, N_A, from which we can calculate the average grain area, *A*. The procedure is to take the square root of *A* and call this the grain diameter, *d*, although this assumes that the cross sectional shape of the grains is a square. The intercept method yields a mean intercept length, L_3. The relationship of this dimension to N_A, *A*, or *d* has not been exceptionally well defined. A variety of planar grain size distribution methods have also been developed to estimate the

number of grains per unit volume, *Nv*, from which the average grain volume, *V*, can be calculated. The relationship between these spatial measures of grain size and the above planar methods has also not been well defined [10].

Committee E-4 has developed a grain size standard for ratings made using semiautomatic or automatic image analyzers (E 1382, Test Methods for Determining the Average Grain Size Using Semi-Automatic and Automatic Image Analysis)[10]. Automated measurements can identify individual grains based upon different gray levels, allowing the computer to sum up the total number of pixels within each grain and therefore providing an area calculation for each individual grain.

The precision and bias of the grain size measurements using either manual or automatic methods depend on the representativeness of the specimens selected and the areas on the plane-of-polish chosen for measurements. For the non-automated procedure, using the intercept method 10 % relative accuracy can be obtain with about 400 intercept counts, while the planimetric method require 700 counts for obtaining the same accuracy. For the semi-automated and- automated procedure, when properly performed, the grain size can be defined to an accuracy of one-tenth a unit with a 95 % confidence and a relative accuracy of 10 %.

Other Measurement Methods

Other standards have been introduced by the ASTM committee E-4 to handle the measurement of occasional very large grains present in an otherwise uniform, fine grain size dispersion (E 930, Methods of Estimating the Largest Grain Observed in a Metallographic Section (ALA Grain Size) or for rating the grain size when the size distribution is non-normal, for example, bi-modal or "duplex" (E 1181, Methods of Characterizing Duplex Grain Sizes). METHODS FOR PREDICTING GRAIN/PHASE GROWTH

There are three categories of models used to predict grain growth in polycrystalline materials. The first category predicts the individual grain size as a function of grain shape. The second category predicts the average grain size as a function of initial grain size, time, and temperature. However, as grain growth proceeds, the value of the average grain size may provide little information if the distribution skews towards extremely large and extremely small grains. The third category of models provides more information on the probability distribution of grain sizes.

Individual Grain Size (Von Neumann's Law)

Von Neumann's Law is a relation between the rate of change of area of an individual cell and its number of sides *n*:

$$\frac{d\mathrm{A}}{dt} = \frac{1}{3} \cdot \pi\sigma k \cdot (n-6) \quad (1)$$

where *k* is the diffusion constant, σ is the specific grain-boundary energy.

This means that a cell with six sides neither grows nor shrinks, although it may change its shape, as diffusion proceeds, until such time as it is involved in a topological change, so that it no longer has six sides. This is particularly important in relation to transient behavior.

Average Grain Size (Isothermal)

The growth rate of the average grain size can be described as [11]:

$$dr/dt = \frac{A_n}{r^n}\left(\frac{r}{r_k} - 1\right) \quad (2)$$

where r_k is the critical radius and A_n will be dependent upon the rate-limiting mechanisms present in the material system. If the coarsening behavior is controlled by the rate of reaction at the grain boundaries, then $n = 1$ and A_n can be described as [12]:

$$A_n = \frac{2\sigma C_\infty V_m^2 K}{vRT} \quad (3)$$

where A_n is average grain area with n sides, σ is the specific grain-boundary energy, C_∞ is the equilibrium concentration at the surface of a precipitate with infinite radius, V_m is the molar volume, K is a constant.

For diffusion-controlled coarsening, the average grain size tends to follow a square root law [1] [13], where $n = 2$. This is particularly true in the case of random orientation distribution. In some systems where diffusion of atoms along the grain boundaries is the controlling factor, it has been found that the following relationship is obeyed [14][15].

$$r^3 - r_0^3 = D \cdot \gamma \cdot x_e \cdot t \quad (4)$$

where r_0 is the mean radius at time $t = 0$, D is the diffusion coefficient, γ is the interfacial energy, x_e is the equilibrium solubility of very large particles, and t is time. Since D and x_e increase exponentially with temperature, the rate of grain coarsening will increase rapidly with increasing temperature [16].

In multiphase systems, it is speculated that grain/phase growth is controlled by diffusion across dislocations. Senkov and Myshlyaev [17] arrived at the following expression for grain coarsening controlled by interphase boundary diffusion, which gives

$$d^4 - d_0^4 = \frac{B_2 \gamma_i V C_0 \delta D_b}{kT} t \quad (5)$$

where d is the average grain diameter, d_0 is the initial grain diameter, B_2 is a geometric constant that includes volume fraction of the second phase, γ_i is the interfacial energy between phase boundaries, V is the molar volume of the second phase, C_0 is the equilibrium solute concentration at the grain boundaries, δD_b is the grain boundary diffusivity, k is the Boltzmann's constant, T is the aging temperature and t is the aging time.

Average Grain Size (Dynamic)

By making certain assumptions regarding the rates of production and annihilation of vacancies, Senkov and Myshlyaev [17] developed a model for dynamic coarsening,

$$d = d_0 + \left(\frac{KB_2\gamma_i VC_0\delta}{kT}\right) t_c \dot{\gamma} [t - t_c + t_c \exp(-t/t_c)] \quad (6)$$

where K is a proportionally constant, t_c is the relaxation time for annihilation of excess vacancies, and $\dot{\gamma}$ is the strain rate.

Grain/Phase Size Distribution

Grain and phase growth in polycrystalline materials develops in time and space in accordance with probabilistic laws and may be due to local variations in the vicinity of individual grains as well as random fluctuation of grain boundaries. In addition, grain growth may have a drift component due to underlying physical processes enforcing changes on the system.

A special class of stochastic[2] processes is called Markov processes. If grain growth is a Markov process, we can calculate the probabilistic density function (PDF) of the size of a particular grain at any time if we know the size at time t. Information about the size before time t does not affect the calculation – the process has no "memory." In continuous time with continuous state space Markov processes are described by the Kolmogorov forward and backward equations (7). The forward equation is also known as the Fokker-Planck (8), (9), (10) diffusion equation.

[2] A process or event that involves the occurrence of random chance events

In grain growth, every grain has the opportunity to grow, shrink or remain at the same grain size. If the grain growth is a Markov process, each of these events is connected with a probability independent of the history of the grain. Consider a grain growth process in discrete time. Let the size, *x*, of particular grain be *Xi* at time *i*. Grain growth is a Markov process if for arbitrary times, n>m>1,

$$px_n\left(x\middle|X_m = y, X_1 = Z\right) = px_n\left(x\middle|X_m = y\right) (7)$$

where $p\,x_n\,(x \mid Xm = y)\,dx$ is the probability that the grain size is within the interval *x, x + dx* at time *n* if the grain size was *y* at time *n*. In general, the Markov process can be defined in terms of the conditional probability density function (PDF) of the grain size.

The Fokker-Planck (3), (4), (5) diffusion equation can describe grain growth if only the size distribution of the grains is considered. Let the probabilities for growth, shrinkage and no change be $\phi_+(x)$, $\phi_-(x)$ and $(1 - \phi_+(x) - \phi_-(x))$ respectively. The corresponding Fokker-Planck equation is:

$$\frac{\partial N_x}{\partial} = \frac{\partial^2}{2\partial x^2}\left(\alpha_x(x,t)\cdot N_x\right) - \frac{\partial}{\partial_x}\left(\beta_x(x,t)\cdot N_x\right) (8)$$

where *x* is the grain size, N_x is the number of grains in the size class $x \rightarrow x+dx$, and $\alpha x\,(x,t)$ and $\beta x\,(x,t)$ are defined by the probabilities for growth and shrinkage.

$$\alpha_x(x,t) = {}_{\Delta x,\Delta}\lim_{t\to 0}\left[\Phi_+ + \Phi_- - \left\{\Phi_+ - \Phi_-\right\}^2\right]\frac{(\Delta x)^2}{\Delta t} (9)$$

$$\beta_x(x,t) = {}_{\Delta x,\Delta}\lim_{t\to 0}\left[\Phi_+ - \Phi_-\right]\frac{\Delta x}{\Delta t} \quad (10)$$

$\alpha x(x,t)$ and $\beta x(x,t)$ are frequently referred to as the stochastic component and drift component of grain growth, respectively [17].

PHASE GROWTH IN SOLDER DURING HIGH TEMPERATURE AGING

Due to the relatively low melting temperature of most tin-based solder systems (lower then 550 K), solder generally operates in a high homologous temperature regime, where $T > 0.5T_M$. Exposure to such high homologous temperatures ultimately leads to a coarsening of the microstructure. Static, isothermal phase coarsening in as-reflowed solder joints is governed by grain interphase boundary diffusion according to the theory by Senkov and Myshlyaev [17].

Rate of grain coarsening is dependent upon the interlamellar spacing. Finer interlamellar spacing creates shorter diffusion distances and the larger volume of phase boundaries through which material diffusion can occur. Interlamellar spacings are dependent upon the tin concentration and the cooling rate. Faster cooling rate and high tin concentrations result in finer lamellar dendrites [21]. As described by Hacke et. al. for eutectic Sn-Pb alloys [18], cooling rates less than ~0.01°C/s, create a equilibrium microstructure consisting of colonies (grains) containing alternating Pb and Sn lamellae (layers of thin plates). With increasing cooling rate the lamellar structure degenerates, leading ultimately to a globular structure of Pb-rich particles dispersed in the Sn-rich phase. Typical solder joints have grain sizes between 2 to 5 microns in diameter, which represents a cooling rate between 1ºC to 0.01ºC/second.

PHASES GROWTH IN SOLDER DURING TEMPERATURE CYCLING

There are two driving forces for solder phase growth during thermo-mechanical cycling (TMC). First, due to its low melting point, the imposed strains during TMC will most likely exceed the elastic limit of the solder and produce plastic deformation. As discussed previously, the presence of plastic deformation leads to the formation of vacancies, which allow for an increased rate of diffusion. In addition, the relatively high solid solubilities of Pb in Sn and vice versa, especially at elevated temperatures, lead to microstructural instability due to coarsening mechanisms. These regions of inhomogeneous

microstructural coarsening are known to be crack initiation sites. It is well documented that these types of microstructures in Sn/Pb alloys fail by the formation of a coarsened band in which a fatigue crack grows.

By studying the microstructural coarsening, which occurs during cyclic loading, constitutive equations for accurately predicting the fatigue life of solder joints can be developed.

While it is well known that phase coarsening occurs in tin-based solders during thermo-mechanical cycling (TMC), few studies have quantified the rate of this effect. Conrad [18], [21], [22], [23], [24], [25] has led a number of investigations on phase coarsening in eutectic solders subjected to TMC. They found that the rate of coarsening was appreciably higher during TMC compared to isothermal annealing, but appear to be governed by the same kinetic interphase boundary diffusion mechanism of Senkov and Myshlyaev [17], with $t^{1/4}$ time behavior. Their results are displayed in Figure 2. It can be seen that the rate of phase growth can appreciably exceed under isothermal conditions. Evans [26] observed similar results, with Evens using the Arrhenius relationship to predict growth rates as a function of temperature. Eventual fatigue life was found to increase with an increasing cooling rate, decreasing grain size, suggesting that the failure event is dependent upon the grain size reaching a critical value. A plot of how microstructural elements in eutectic solder change with cooling rate is shown in Figure 3.

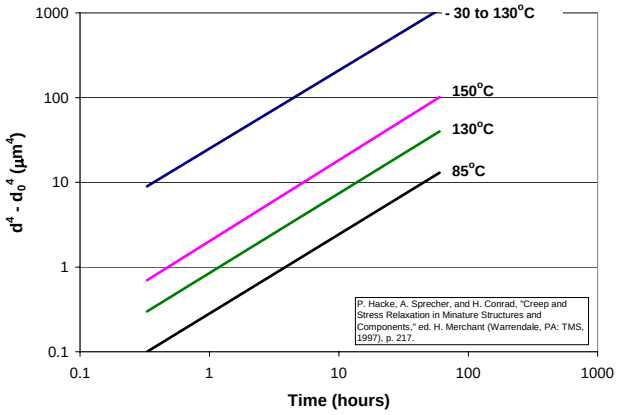

Figure 2 Phase growth in solder during temperature cycling

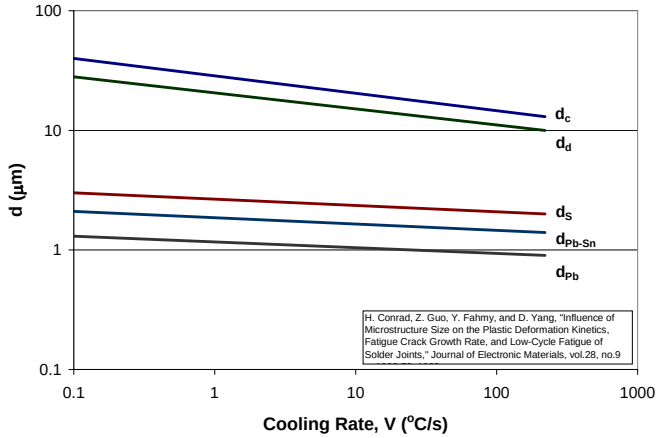

Figure 3 Log-Log/plot of the size of the various various micro-constituents vs. reflow cooling rate for eutectic Sn-Pb alloy solder joints. Dc=colony, dd=Pb dendrite, d_{Sn}=eutectic Sn phase, d_{Pb}=eutectic Pb phase and $d_{Pb\text{-}Sn}$=(d_{Pb+dSn})/2=average eutectic phase size.

Frost investigated the microstructural evolution of Pb-rich solders [21] [27]. They found that if the maximum temperature during TMC exceeds the solvus temperature and the frequency of thermal cycling is high enough, the competing processes of dissolution and precipitation might be such that the microstructure may eventually reach some steady state.

DISCUSSION

Characterization of solder microstructure and understanding of phase growth behavior requires the use of appropriate techniques and understanding of current theories. A varied selection of etchants and etching techniques allow for clear observation of the various microstructural elements within the solder interconnect. Use of automated grain/phase measurement, which is rapidly replacing traditional manual methods, should be tempered with the realization of the limitation of the ability of two-dimensional measurements to detail three-dimensional objects.

Accurate detailing of phase morphology allows for the use of grain growth models to potentially develop acceleration factors. Within traditional grain growth studies, acceleration factors have been used to predict grain diameter as a function of temperature and time of exposure. Based on the observations by Conrad, Evans and Frost, changes in phase diameter may potentially be used to correlate temperature cycling environments of two different magnitudes.

Plotting changes in phase size during accelerated testing and comparing results to microsectional analysis of field units does provide the opportunity to calculate an acceleration factor. However, there are a number of limitations to this approach. It requires that the test and field units have exactly the same part types and the acceleration factor can only be calculated after the test has been completed.

Because the rate of phase growth is dependent upon the amount of stress applied during thermo-mechanical cycling, a more powerful use of phase coarsening studies would be in combination with that to determine an acceleration factor and design damage models [29]. Solder joint phase size measurements could then be used to validate the results of the modeling.

REFERENCES

[1]. Atkinsen, H. V. “Theories of Normal Grain Growth in Pure Single Phase Systems,” Acta Met., V. 36 (1988), pp.469-491.

[2]. K. Lucke, G. Abbruzzese, and I. Heckelmann, “Statistical Theory of 2-D Grain Growth Based on First Principles, and its Topological Foundation”, Mat. Sci. Forum 94 (1992), pp. 1-16.

[3]. H. Abubauer, "Acceleration of Coarsening by Cycling of Temperatures," Scripta Metallurgica, vol. 12, pp. 1003-6, 1978.

[4]. Metals Handbook, 9th edition, Vol. 9, Metallography and Microstructures, American Society for Metals, 1985, pp. 450

[5]. www.metallographic.com, Feb. 2002, PACE Technologies

[6]. K.-N. Tu, UCLA (2001)

[7]. Empfasis, July 2001, Nat. Elec. Manuf. Center of Excellence

[8]. Grains - Quantitative Metallographic Analysis; 2001 Soft Imaging System GmbH

[9]. E 112, paragraph 12

[10]. ASTM Committee E-4 and Grain Size Measurements

[11]. R. Vengrenovitch, "On the Ostwald Ripening Theory," Acta. Metall., vol. 30, pp. 1079-86, 1982.

[12]. C. Wagner, Z. Elektrochem., vol. 65, p. 581, 1961

[13]. P. Feltham, "Grain Growth in Metals," Acta. Metall., vol. 5, pp. 97, 1957.

[14]. M. Speight, "Growth kinetics of grain–boundary precipitates" Acta. Metall., vol. 16, pp. 133, 1968

[15]. H. Kirchner, "Cumulative distribution functions during particle coarsening," Metallography, vol.4, no.4 p. 297-302, 1971

[16]. Li-Lei Ye, Zonghe Lai, Johan Liu and A. Thoelen; “.Microstructural coarsening of lead free solder joints during thermal cycling”; 2000 Electronic Components and Technology Conference.

[17]. O. Senkov and M. Myshlyaev, "Grain growth in a superplastic Zn-22%Al alloy," Acta Metallurgica, vol.34, no.1 p. 97-106, Jan. 1986

[18]. P. Hacke, Y. Fahmy, and H. Conrad, "Phase Coarsening and Crack Growth Rate During Thermo-Mechanical Cycling of 63Sn37Pb Solder Joints"; Journal of Electronic Materials, vol.27, no.8 p. 941-7; Aug. 1998

[19]. S. Kailasam; M.E. Glicksman; S.S. Mani; and V.E. Fradkov; "Investigation of Microstructural Coarsening in Sn-Pb Alloys"; Metallurgical and Materials Transactions A, vol.30A, no.6 p. 1541-7; June 1999

[20]. R. Chnchani; "Modeling and Simulation – The Effect of Grain Coarsening on Local Stresses and Strains in Microstrure"; Sandia national Labs

[21]. H. Frost, G. Stone, and R. Howard, "The Effects of Thermal History on the Microstructure and Mechanical Properties of Solder Alloys," Microelectronic Packaging Technology, Materials and Processes. Proceedings of the 2nd ASM International Electronic Materials and Processing Congress, Philadelphia, PA, USA; 24-28 April 1989, p. 121-7

[22]. P. Hacke, A. Sprecher, and H. Conrad, "Computer Simulation of Thermo-Mechanical Fatigue of Solder Joints Including Microstructure Coarsening," Trans. ASME J. Electronic. Pkg., vol. 115, no.2, pp. 153-58.

[23]. P. Hacke, A. Sprecher, and H. Conrad, "Creep and Stress Relaxation in Miniature Structures and Components", ed. H.D. Merchant (Warrendale, PA: TMS, 1997), p. 217

[24]. P. Hacke, A. Sprecher, and H. Conrad, "Microstructure coarsening during thermomechanical fatigue of Pb-Sn solder joints," J. Elect. Mater., vol. 26, no. 7, pp. 774-82, 1997.

[25]. H. Conrad, Z. Guo, Y. Fahmy, and Di Yang; "Influence of Microstructure Size on the Plastic Deformation Kinetics, Fatigue Crack Growth Rate, and Low-Cycle Fatigue of Solder Joints"; Journal of Electronic Materials, vol.28, no.9 p. 1062-70; 1999

[26]. W. Engelmaier, "The changeable structure of solder joints", Global SMT & packaging, Vol.4, no.1, Dec/Jan. 2003/4. p.31-32.

[27]. H. Frost and R. Howard, "Creep Fatigue Modeling for Solder Joint Reliability Predictions Including the Microstructural Evolution of Solder," IEEE CHMT, vol. 13, no. 4, Dec. 1990, pp. 727-35.

[28]. J. H. L. Pang, Kwang Hong Tan, Xunqing Shi, and Z. P. Wang; "Thermal Cycling Aging Effects on Microstructural and Mechanical Properties of a Single PBGA Solder Joint Specimen"; IEEE Transactions On Components And Packaging Technologies, vol. 24, no. 1, March 2001.

[29]. A Demonstration of Virtual Qualification for the Design of Electronic Hardware, J. Cunningham, R. Valentin, C. Hillman, A. Dasgupta, and M. Osterman, ESTECH 2001, IEST, Phoenix, AZ, April 2001.

DISCLAIMER

DfR represents that a reasonable effort has been made to ensure the accuracy and reliability of the information within this report. However, DfR Solutions makes no warranty, both express and implied, concerning the content of this report, including, but not limited to the existence of any latent or patent defects, merchantability, and/or fitness for a particular use. DfR will not be liable for loss of use, revenue, profit, or any special, incidental, or consequential damages arising out of, connected with, or resulting from, the information presented within this report.